Environmental Science & Technology

Article

pubs.acs.org/est

Controls on Soluble Pu Concentrations in PuO_2/Magnetite Suspensions

Andrew R. Felmy,*[,†] Dean A. Moore,[†] Carolyn I. Pearce,[†] Steven D. Conradson,[‡] Odeta Qafoku,[†] Edgar C. Buck,[†] Kevin M. Rosso,[†] and Eugene S. Ilton[†]

[†]Pacific Northwest National Laboratory, Richland, Washington, United States

[‡]The Los Alamos National Laboratory, Los Alamos, New Mexico, United States

Supporting Information

ABSTRACT: Time-dependent reduction of PuO_2(am) was studied over a range of pH values in the presence of aqueous Fe(II) and magnetite (Fe_3O_4) nanoparticles. At early time frames (up to 56 days) very little aqueous Pu was mobilized from PuO_2(am), even though measured pH and redox potentials, coupled to equilibrium thermodynamic modeling, indicated the potential for significant reduction of PuO_2(am) to relatively soluble Pu(III). Introduction of Eu(III) or Nd(III) to the suspensions as competitive cations to displace possible sorbed Pu(III) resulted in the release of significant concentrations of aqueous Pu. However, the similarity of aqueous Pu concentrations that resulted from the introduction of Eu(III)/Nd(III) to suspensions with and without magnetite indicated that the Pu was solubilized from PuO_2(am), not from magnetite.

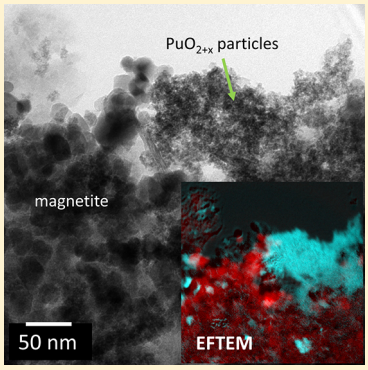

INTRODUCTION

The mobility of Pu in subsurface groundwaters is influenced by a variety of factors including aqueous complexation, sorption to solid phases, and redox state. It has long been known that Pu as Pu(IV) is only sparingly soluble as PuO_2(am) except under very acidic conditions, and that the principal soluble forms of Pu under environmentally relevant conditions are either Pu(V) or Pu(III).[1−3] More studies have focused on the reduction of Pu(V) to Pu(IV)[4−8] compared to the reduction of Pu(IV) to Pu(III).[9,10] The latter experiments are complicated by the presence of high total Pu concentrations, due to the presence of solid phase PuO_2, which promotes solution radiolysis and a consequent evolution in measured pH values and redox potentials. Such processes could occur in the near field nuclear waste package environment where PuO_2 is present along with a solid form of Fe(II) such as magnetite, Fe_3O_4, a common carbon steel corrosion product.[11,12] The reduction of PuO_2(am) by aqueous Fe(II) has been studied both in the initial absence[9,10] and presence of Fe(III) oxides (i.e., goethite[10]). However, to the best of our knowledge, reduction of PuO_2(am) by Fe(II)-bearing solid phases has not been directly targeted, even though such solids are ubiquitous in environmental systems (and as corrosion products). In fact, one of the principal reaction products that can form in the Fe(II)/Fe(III)−PuO_2(am) system is magnetite:

$$2PuO_2(am) + 3Fe^{2+} \leftrightarrow Fe_3O_4(magnetite) + 2Pu^{3+} \quad (1)$$

If such reactions occur, because of the higher thermodynamic stability of crystalline products such as magnetite relative to amorphous forms in general, there is the potential to appreciably increase the concentration of soluble Pu(III) over that which would be predicted to form if the Fe(III) reaction product were ferrihydrite (Figure 1). Factors that affect the precipitation pathway and the identity of the Fe(III) products are thus expected to strongly influence the PuO_2 reduction extent. Proof of concept was provided in our previous work,[10] where the introduction of goethite, a more stable phase than ferrihydrite, facilitated increased reduction of PuO_2(am) ostensibly by acting as a structural template for growth of a goethite-like phase, effectively bypassing relatively metastable ferrihydrite as the Fe(III) product. This illustrated the thermodynamic importance of the nature of the Fe(III) reaction product in the heterogeneous reduction of PuO_2(am) by Fe(II).

In the present study we compared the reduction of PuO_2(am) by Fe(II)(aq) in the absence and presence of magnetite (Fe_3O_4) nanoparticles. Magnetite was selected in part because eq 1 is thermodynamically favored under most environmentally relevant conditions, and in part because it is an end member of the titanomagnetite series found in Pu contaminated sediments at the Hanford site.[13] Further, these magnetite nanoparticles are routinely synthesized in our laboratory and have been carefully characterized and used in previous heterogeneous electron transfer studies.[14,15]

Received: November 3, 2011
Revised: September 17, 2012
Accepted: September 27, 2012
Published: September 27, 2012

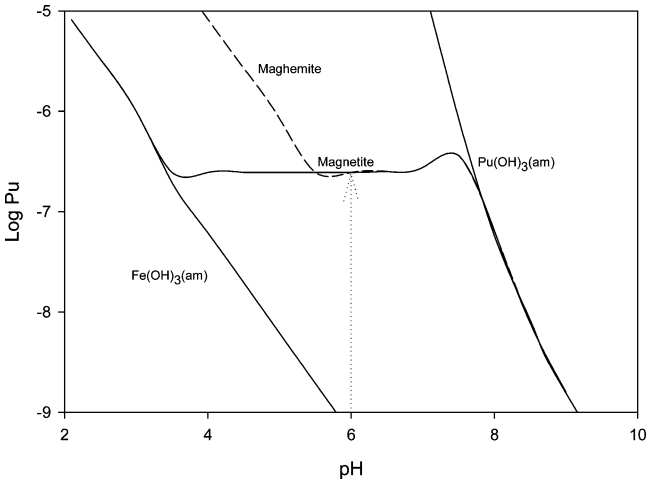

Figure 1. Calculated Pu(III) concentrations in equilibrium with PuO_2(am) with different Fe(III) reaction products and at an Fe(II) concentration of 0.001 M. The arrow indicates the possible increase in Pu(III) concentration if the Fe(III) reaction product were magnetite rather than ferrihydrite.

METHODS AND MATERIALS

The methods and materials for the preparation of the PuO_2(am) and Fe(II) solutions were similar to those used by Felmy et al.[10] and are described here briefly. All reagents were analytical and reagent grade. All solutions were prepared with distilled–deionized (DDI) water and stored under an argon atmosphere. A 106 g/L Pu stock solution was prepared in 8 M HNO_3 consisting of Pu^{239} (93.3%) and Pu^{240} (6.5%) along with small concentrations of Pu^{241} (0.1%), Pu^{238}(0.02%), and Pu^{242} (0.05%). The stock solution was prepared and purified from daughter products at the start of the study (6/2010). UV–vis spectra of the solution showed only Pu(IV). A standard CO_2-free NaOH solution (6.45 M) was prepared by dissolving a calculated amount of solid NaOH (Anachemia Acculute) and titrating with standard 6.0 M HCl solution (GFS Chemicals Inc.). Stock solutions of 0.25 M $KBrO_3$ and 0.6 M $FeCl_2$ in 0.001 M HCl were prepared by dissolving solid $KBrO_3$ and $FeCl_2{\cdot}4H_2O$ in DDI water, respectively. A 0.5 M thenoyltrifluoroacetone (TTA) stock solution in toluene was prepared for use in oxidation state analysis and stored in an amber bottle. The TTA was purified by heating approximately 20 g of TTA to 42–44 °C under vacuum with a cooling tube to condense the purified TTA.

All experiments were conducted at room temperature (23 ± 2 °C) in a controlled atmosphere chamber of prepurified Ar (99.99%) with <1 ppm O_2. PuO_2(am) was prepared from the nitrate solution by adding an aliquot of the stock solution to a small volume of DDI water and then adjusting the pH to approximately 10 using the NaOH stock solution. The resulting suspension was aged overnight in the mother liquor. The suspension was then centrifuged (at 2000*g* for 10 min), the supernatant was removed and the precipitate was washed twice with 20–30 mL of DDI water to remove nitrate. The suspensions were centrifuged after each addition of DDI water. The final PuO_2 precipitate was suspended in water and stirred vigorously.

Magnetite nanoparticles were prepared via an ambient temperature synthesis from a stoichiometric mixture of $FeCl_2$ and $FeCl_3$ in a 0.3 M HCl (pH < 1) solution under anoxic conditions.[14−17] All solutions used during the preparation of the magnetite nanoparticles were prepared inside a N_2 environmentally controlled chamber and additionally bubbled with N_2, where all N_2 gas was from a liquid nitrogen boil-off supply. The procedure consisted of quickly adding the stoichiometric Fe(II)/Fe(III) mixture to a 25% w/v ammonium (NH_4OH) solution while vigorously (800 rpm) stirring the base, leading to instantaneous precipitation of magnetite nanoparticles according to the following equation:

$$Fe^{2+} + 2Fe^{3+} + 8OH^- \rightarrow Fe_3O_4 + 4H_2O \quad (2)$$

Although the precipitation of magnetic black precipitate was observed immediately after the addition of Fe-solution, the

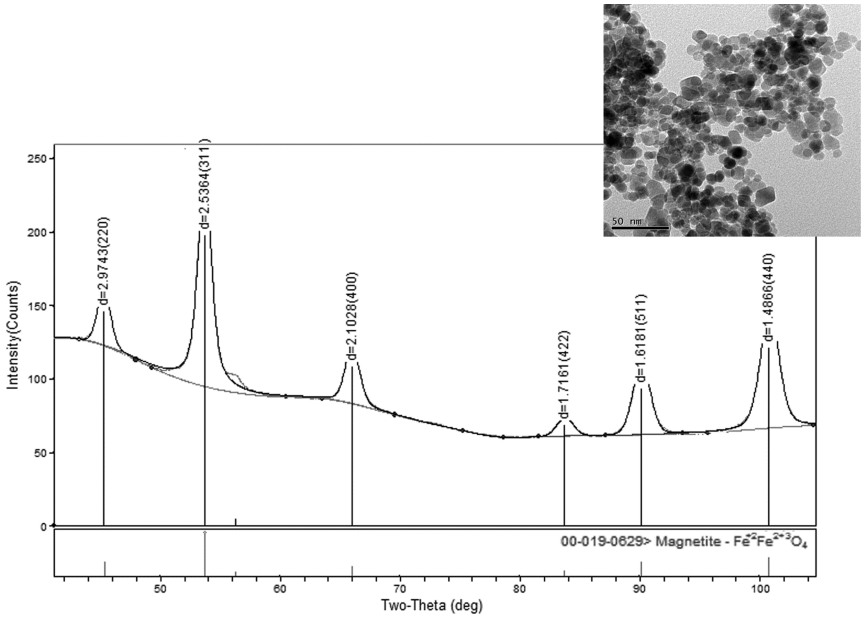

Figure 2. XRD pattern of nanomagnetite starting material. The significant peak broadening is consistent with an average particle size of 10 nm. The insert shows a TEM image of the magnetite particles before reaction.

suspension was stirred for additional 30 min. The solid phase was magnetically separated from the aqueous phase, washed three times with deionized degassed water to remove the excess salts, and resuspended in deionized water (pH ~8.5). The suspension was stored in the environmental chamber for further use. Suspension density (9.32 g L^{-1}) was calculated by drying 1-mL aliquots of liquid suspension, in triplicate, in an oven at 60 °C for 24−48 h until there was no change in mass. One-mL aliquots of the suspension were also digested, in triplicate, in 5 M HCl to determine Fe(II)/Fe(III) ratio of the solid. Determination of Fe(II) was done using the ferrozine method.[18] The Fe(III) concentration was calculated by subtracting the Fe(II) concentration from the total Fe measured using an Agilent 7500 ICP-MS. Based on the digestion analysis the stochiometric formula for the magnetite nanoparticles was calculated to be $Fe_{1.02}^{2+}Fe_{1.98}^{3+}O_4$. Transmission electron microscopy (Jeol-JEM 2010) revealed nearly spherical ~12-nm particles (Figure 2). The N_2-BET (Quantachrome Autosorb 6-B) determined surface area of the freeze-dried nanomagnetite was 98.2 m^2 g^{-1}. Micro X-ray diffraction of the anoxic nanoparticle suspension (Rigaku D/Max Rapid II) revealed that magnetite was the only crystalline phase present and the small size of the crystallites yielded broad peaks (Figure 2). Cell refinement was carried out in JADE using a cubic magnetite (Fe_3O_4) structure (PDF 00-019-0629) as the starting model to determine lattice parameter (8.406 Å) and crystallite particle size (10 nm), which is in very good agreement with the TEM analysis.

Aliquots of the PuO_2(am) suspension containing approximately 2 mg of Pu were pipetted into 25-mL centrifuge tubes and the solutions were made to 0.001 M $FeCl_2$ and 0.015 M NaCl. Approximately 3 mg of magnetite was then added to each suspension. The pH was adjusted to a range of values initially between 7 and 10.3. Three different sets of suspensions were prepared in this way. In the first set (Set I), 12 PuO_2(am)/magnetite suspensions were prepared along with four 0.001 M $FeCl_2$ solutions in 0.015 M NaCl, without added PuO_2, to serve as controls for Fe(II) oxidation by chamber gases. A second set of suspensions (Set II) was prepared to test for possible differences in reduction between samples in both glass and polycarbonate centrifuge tubes and, eventually, as we will describe under Results and Discussion, test for possible Pu(III) sorption by adding different concentrations of Eu(III)/Nd(III) as competitive cations. A total of four suspensions at different pH values were prepared as part of Set II. Finally, a third set of suspensions (Set III) was prepared in a fashion similar to Set II except two different concentrations of added PuO_2 were used in the presence of Nd(III) to examine the impact of solids concentration on Pu displacement. A total of eight suspensions at different pH values were prepared as part of Set III.

The PuO_2(am)/magnetite suspensions and $FeCl_2$ controls were sampled at timed intervals for pH and Eh measurements. The samples were then centrifuge filtered at 2000*g* for 10 min using 30 000 molecular weight cutoff Pall Microsep filters.

The filters were pretreated by passing 2 mL of pH-adjusted DDI water (at the pH of the sample) through each filter followed by 0.5 mL of sample to saturate any adsorption sites. This filtrate was discarded. Sufficient sample was then filtered and split into four fractions for total Pu analysis, oxidation state determination by solvent extraction, and Fe(II) analysis. Total Pu in one fraction was determined by liquid scintillation counting using a Wallac 1414 WinSpectral and Packard Hionic Fluor cocktail. Since Pu(aq) was below detection limits for spectroscopic determination, Pu oxidation states were determined by thenoyltrifluoroacetone (TTA) extraction. In this procedure Pu(IV) was determined in one subsample by TTA extraction and Pu(IV) plus Pu(III) in another subsample which included $KBrO_3$. $KBrO_3$ oxidizes Pu(III) to Pu(IV) but not to higher oxidation states. The TTA was allowed to equilibrate with chamber gases in order to remove O_2 that could oxidize Pu(III), as described in our earlier study.[10] A fourth fraction was used for Fe(II) analysis. The Fe(II) was analyzed with a Hach DR2800 spectrophotometer at 562 nm inside the chamber using the ferrozine method.[18] In our final set of experiments (Set III), which contained added Nd(III), additional filtered samples were collected and the potential for the presence of colloidal Pu in the filtered samples was examined using trichloroacetic acid (TCA) in *n*-octanol according to the procedure of Wilson et al.[19] The TCA in *n*-octanol was prepared immediately before use to ensure good sample recovery (R. Wilson, personal communication). Analysis of several stock solutions containing different total Pu concentrations and different oxidation state distributions showed that the total Pu concentrations were accurately determined even to low concentration (typically ±1%). However, as expected oxidation state determinations were not as accurate typically ±5% except in the cases where one oxidation state was at low concentration (i.e., <10% of the total Pu) in which cases errors could be 20−30% owing to the low count rates.

The pH of solutions was measured with a Beckman model 71 pH meter equipped with an Orion-Ross semi-Micro combination glass electrode, and the Eh was measured using a Broadley-James redox platinum electrode. Before each sampling, the Eh probe was calibrated using pH 4 and pH 7 buffer solutions saturated with quinhydrone. The Eh buffer readings were made both before and after sampling to test for probe stability. In the Eh measurements 2- and 5-min readings were recorded for each sample. However, in solutions of low Fe(II) content the redox potentials were poorly poised and the measured potentials exhibited considerable drift. In such cases the potentials were recorded only after reaching a steady state.

After the last sampling (321 days) of the PuO_2(am)/magnetite suspensions in Set I, there was an opportunity to examine a limited number of the remaining solid fractions by X-ray absorption fine structure (XAFS) spectroscopy. However, the continuing radiolysis of the solutions reduced the pH of most of the samples to the acidic range where magnetite is not stable. Only the samples at the highest pH (>8) with added magnetite and the samples with added Eu(III) maintained pH values greater than 7 where magnetite is expected to remain stable.

Pu L_3 XAFS spectra of these selected samples were measured at the Stanford Synchrotron Radiation Laboratory (SSRL) on end station 11-2. Si [220] crystals were used to monochromate the beam. The relative orientation of the crystals was set to maximize the beam intensity (fully parallel), harmonics were rejected with a flat, Rh-coated glass mirror tilted to have a cutoff energy of 22−23 000 keV. Spectra were calibrated by defining the first inflection point of a Zr foil measured within the Pu L_3 scans as 17999.35 eV, and the ionization energy (k = 0 $Å^{-1}$) as 18062 eV. The spectra were measured in the fluorescence mode using 24 elements of a 32 element Ge detector and XIA digital amplifiers windowed on the L_α emission. All Fourier transforms were calculated using a sine window function.

Metrical parameters were obtained by nonlinear least-squares curve-fits of the EXAFS using amplitudes and phases calculated by the Feff 7 code, which we find more accurate than Feff 8 for these atom pairs.

Selected PuO_2(am)/magnetite solids (Set I) were also analyzed by transmission electron microscopy (TEM) after 321 days of reaction using a FEI (Hillsboro, OR) Tecnai $G^2$30 field emission gun TEM operated at 297 keV and equipped with a Gatan (Pleasanton, CA) Orius digital camera and Gatan image filter (GIF2000) for electron energy-loss spectroscopy. Diffraction patterns, electron energy-loss spectra, and electron micrographs were analyzed with Gatan DigitalMicrograph 1.83.842 and aided with custom scripts from Mitchell (2005).[20]

Equilibrium thermodynamic data for aqueous Fe(II) hydrolysis species were calculated from the hydrolysis constants given by Martell and Smith[21] and for Fe(III) species by using the hydrolysis constants from the recent review by Stefansson.[22] Thermodynamic data for magnetite were taken from the review by Robie and Hemingway.[23] The equilibrium constants for Pu(III) hydrolysis species are from the compilation of Felmy and Rai.[24] All other thermodynamic data for Pu(III), Pu(IV), and Pu(V) species are from the compilation of Lemire et al.[25] (see Table S1 in the Supporting Information). The calculations were performed using the GMIN computer program,[26] which includes Pitzer ion-interaction parameters from the tabulation of Felmy and Rai.[24] However, because our solutions were relatively dilute (ionic strength ~0.015) the ion-interaction parameters do not contribute significantly to the final calculated activity coefficients, and the Pitzer formalism therefore reduced to Pitzer's form of the extended Debye–Hückel equation.

This thermodynamic model was used to calculate aqueous Pu(III) concentrations assuming equilibrium between different iron-containing solid phases and the measured aqueous Fe(II) concentration (e.g., Reaction 1). Thermodynamic modeling was also used to help interpret the measured pe and pH measurements in terms of possible equilibrium with Pu or iron-containing solid phases. For example, the aqueous Pu(III) concentration can be calculated assuming equilibrium of the solutions with PuO_2(am) (e.g., Reaction 2):

$$PuO_2(am) + 4H^+ + e^- = Pu^{3+} + 2H_2O \quad (3)$$

where log K° = 15.7 ± 1.0, calculated from the data of Lemire,[25] and the calculated activity coefficient for aqueous Pu(III) is 0.28. The log K° of 15.7 ± 1.0 is in good agreement with log K° of 15.5 proposed by Rai et al.,[9] log K° of 15.4 ± 0.5 in Guillamont et al.,[27] and log K° of 15.4 ± 0.5 in Neck et al.[28]

RESULTS AND DISCUSSION

Total aqueous Pu concentrations in PuO_2(am)/magnetite suspensions showed very low total Pu concentrations in solution (Figure 3, Table S2) during the first sampling period, at 22 days. In fact, only two samples showed total Pu concentrations significantly above the analytical detection limit of approximately 10^{-10} M. In these samples aqueous Pu appears to be present predominately as Pu(III) (Table S2). However, the aqueous Pu(III) concentrations in these samples were much lower than would be predicted using the pH and pe measurements (see Figure 3).

The aqueous Pu concentrations determined in samples taken at the 56-day study period continued to show relatively low concentrations that were in general below the values predicted

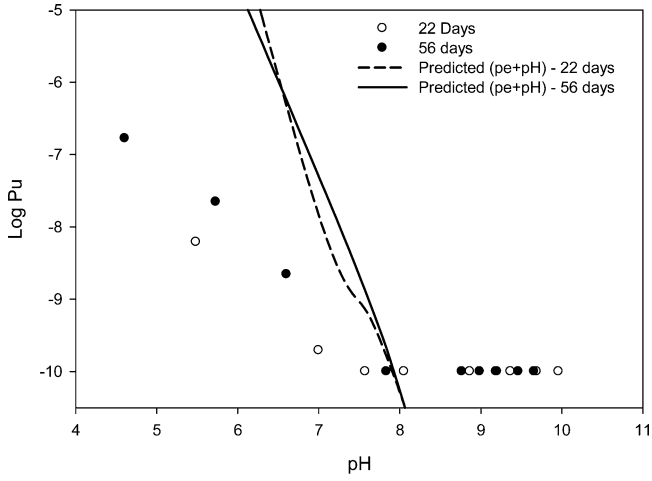

Figure 3. Set I: Aqueous Pu concentrations measured in PuO_2(am)/magnetite suspensions at early time frames. Lines indicate calculated Pu(III) concentrations using measured pe and pH values.

using the measured pH and pe values (Figure 3). These same concentrations were also significantly below the concentrations predicted assuming equilibrium with PuO_2(am) and magnetite as the Fe(III)-containing reaction product (see eq 1 and Figure 4). This same trend of lower aqueous Pu concentrations than

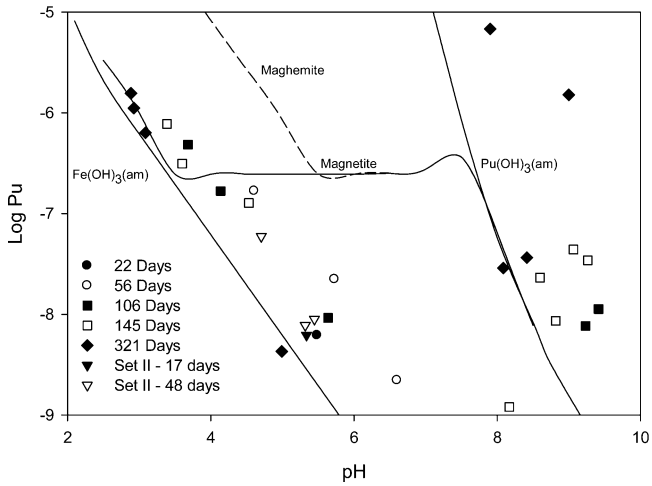

Figure 4. Aqueous Pu concentrations measured in PuO_2(am)/magnetite suspensions without added Eu(III)/Nd(III). Calculated curves use data on the aqueous Fe(II) concentration along with the indicated Fe(III)-containing reaction product in the thermodynamic modeling.

predicted by equilibrium with PuO_2(am) and magnetite continued during all sampling periods, extending to the final sampling period of 321 days (Figure 4). In fact, the aqueous Pu concentrations gradually decreased with time at similar pH values until at 321 days they became similar to predictions assuming equilibrium with PuO_2(am) and ferrihydrite as the Fe(III)-containing reaction product (Figure 4). This observation is consistent with the gradually increasing pe values and lower Fe(II) concentrations measured in the samples with time (Tables S2–S6) and indicates the solutions gradually became more oxidizing. The decrease in pe values and Fe(II) concentrations was not observed in control samples, data not shown, which contained the same aqueous Fe(II) concen-

trations but no PuO_2(am) or magnetite, indicating that the increase in oxidation potential was related to radiolysis rather than trace O_2 in the chamber gases.

The aqueous Pu concentrations in samples at very high pH > 8.5 showed unexpected high concentrations. In fact, the Pu concentrations are higher than would be predicted assuming all of the soluble Pu was Pu(III) and equilibrium with $Pu(OH)_3$(am). Unfortunately, oxidation state analysis of these samples, Tables S4 and S6, was not conclusive owing to poor sample recovery during the oxidation state determination (i.e., significantly less than 100% of the total Pu was accounted for in the combined oxidation state determination steps). Since the total Pu observed in these studies exceeded the concentrations predicted from equilibrium with $Pu(OH)_3$(am), we assume that a significant fraction of this aqueous Pu was present as oxidized Pu(V/VI).

TEM examination of one of these high pH samples (pH = 8.085 in Table S6) following the 321-day sampling period revealed nanosized particles of partially amorphous plutonium oxide and magnetite particles. The Pu and Fe phases were separated as colloidal aggregates. XAFS analysis shows a lower Pu−Pu backscatter and a broad backscatter at long distances indicating a disordered Pu distribution within the solid relative to other PuO_{2+-} phases examined previously.[29] XANES analysis does not show any indication of Pu(III) in the solid phase (detection limit is 5−10% of the solid).

The aqueous Pu concentrations in Set II in both the 17-day and 48-day samplings, which were performed in both glass and plastic centrifuge tubes (Tables S7−S8 and Figure 4), are similar to the Set I results. This demonstrated that possible dissolution of silica from the glass and sorption onto the solids, which could have occurred at the higher pH values, or sorption of Pu to the container walls did not impact the aqueous Pu concentrations.

Eu(III)/Nd(III) Additions. The measured pH and pe values in several samples at early time frames (22 days and 56 days) described above indicated the potential for significantly higher reduction of PuO_2(am) to Pu(III) than analytically measured. Although such high Pu(III) concentrations were not observed in the aqueous phase, it is possible that significant amounts of Pu(III) could have been sorbed to the surface of the magnetite nanoparticles, as suggested by recent observations of the reduction of Pu(V) to Pu(III) on the surface of magnetite.[4] Trivalent lanthanides such as Eu(III) or Nd(III) are analogs for trivalent actinides[24,30,31] and would be expected to compete with Pu(III) for sorption sites. Hence, aqueous Eu(III)/Nd(III) was added to selected suspensions in an effort to displace any sorbed Pu(III) from magnetite surfaces.

Eu(III) was first added to three selected samples in Set I (Table S3) following the 22-day sampling period. The introduction of high concentrations of Eu(III), 0.01 M, caused an increase in the solution pH to values around 8 (Table S3). The higher pH resulted in much lower aqueous Pu concentrations, and we were unable to directly observe any displacement of Pu(III) from the solid phase. After adjusting the pH of these samples by adding small amounts of HCl, the suspensions were resampled at the 106-, 145-, and 321-day study periods (Tables S4−S6). The results showed elevated aqueous Pu concentrations relative to samples without added Eu at similar high pH values indicating that Pu was displaced into solution. However, the lower pH samples showed total aqueous Pu concentrations very similar to the values found in suspensions without added Eu(III).

To gain more insight, the Set II suspensions were spiked with Eu(III) or Nd(III) at lower total concentration (0.001 M) and then resampled immediately after the addition of the Eu(III)/Nd(III). Nd(III) was also used to test for any possible differences between the two trivalent lanthanides. The use of a lower total trivalent lanthanide concentration did not result in dramatic changes in pH. The results, given in Figure 5 and

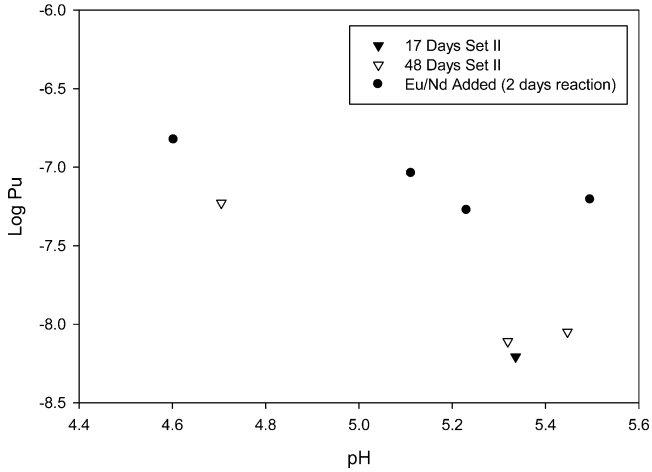

Figure 5. Aqueous Pu concentrations measured in PuO_2(am)/magnetite suspensions in Set II before and after the addition of Eu(III)/Nd(III).

Table S9, showed approximately an order of magnitude increase in the aqueous Pu concentration after only 2 days of reaction at similar pH values. Oxidation state analysis of these Pu samples showed a large fraction of the aqueous Pu is Pu(III), indicating that at least a significant fraction of the solubilized Pu is Pu(III).

Although the aqueous Pu clearly and rapidly increased in these samples following the introduction of Nd(III)/Eu(III), it was not conclusive that the solubilized Pu came from the surface of magnetite. To test this possibility we set up a series of PuO_2(am) suspensions in the presence of aqueous Eu(III) and Fe(II), but no magnetite, at the same concentrations used in Set II described above. These suspensions were sampled after 29 and 140 days of equilibration (see Tables S10 and S11). The aqueous Pu concentrations in these suspensions also showed high aqueous Pu concentrations. In fact, the aqueous Pu concentrations in these samples were very similar to the concentrations observed in the suspensions that contained both PuO_2(am) and magnetite. This suggests that the increase in aqueous Pu concentrations following the addition of Eu(III)/Nd(III) was related to displacement of Pu from the surface of PuO_2(am) rather than from the surface of magnetite. In fact, a detailed comparison of all of the data in the presence of Eu(III)/Nd(III) shows a very consistent trend of nearly identical aqueous Pu concentrations despite the differences in added Eu(III)/Nd(III), pH adjustments, and the presence or absence of magnetite (Figure 6). Hence, any Pu(III) adsorbed to magnetite did not contribute significantly to the solubilized Pu. Further, comparison with the data of Rai et al.[9] (no added Eu/Nd and magnetite, just PuO_2) clearly shows that the introduction of trivalent ions into the PuO_2/magnetite suspensions increased the Pu concentration in solution by solubilizing Pu from the PuO_2(am) (Figure 6).

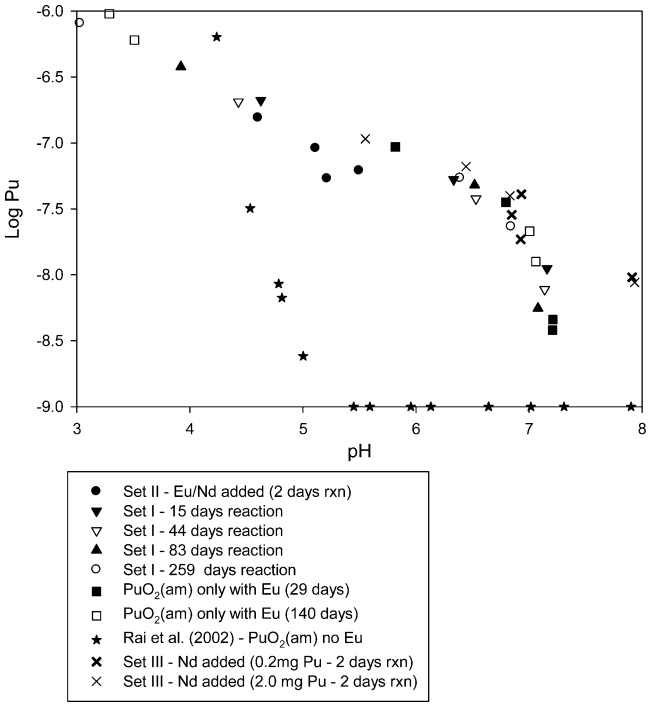

Figure 6. Aqueous Pu concentrations measured in PuO_2(am)/magnetite suspensions in the presence and absence of Eu(III)/Nd(III).

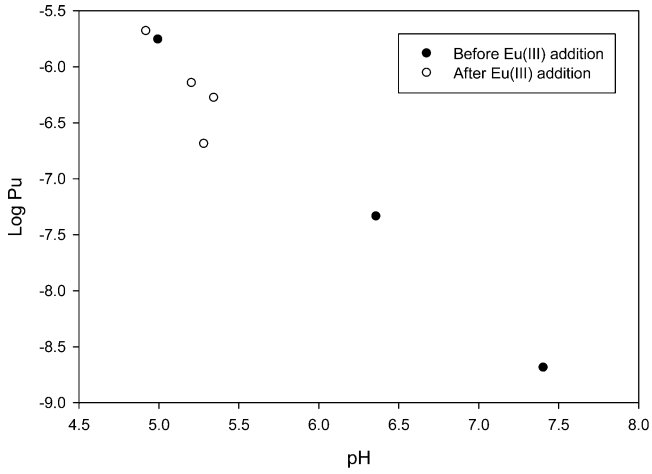

Figure 7. Comparison of aqueous Pu concentrations in PuO_2(am) suspensions before and after the addition of Eu(III) in the absence of aqueous Fe(II) and magnetite. Oxidation state analysis indicated that the aqueous Pu was almost exclusively nonextractable in TTA.

The oxidation state analysis of the aqueous Pu concentrations in the PuO_2(am) suspensions without magnetite shows the presence of significant concentrations of nonextractable Pu (Tables S10–S12). The presence of nonextractable Pu after reaction indicates that displaced Pu could be partially oxidized to Pu(V/VI) following reaction. As a partial test we analyzed the filtrates from Set III samples which contained only PuO_2 and Nd(III) using the recently published TCA in *n*-octanol extraction procedure of Wilson et al.[19] which is selective for Pu colloids. The results (Table S12) show that the filtered samples contain very few if any colloidal Pu particles, indicating the nonextractable Pu in these samples is soluble Pu(V/VI). Further, we examined PuO_2(am) suspensions before and after the addition of Eu(III) but in the absence of aqueous Fe(II) and magnetite. The results, Figure 7, show that the addition of Eu(III) did increase the aqueous Pu concentration, but that this increase was directly related to the decrease in pH resulting from the addition of the Eu(III) spike and that nearly all aqueous Pu was nonextractable in TTA. Specifically, the aqueous Pu concentrations at the same pH values were nearly identical both before and after the addition of Eu(III). This contrasts strongly with the behavior of the system under reducing conditions, where addition of Eu/Nd increased aqueous Pu relative to systems at the same pH without added Eu/Nd.

It is also of interest to discuss the processes that might control the aqueous Pu concentrations in the samples with added Eu/Nd. First, although the Pu concentrations have increased substantially over the values in the absence of Eu/Nd the Pu concentrations are still about an order of magnitude lower than that predicted by equilibrium between PuO_2(am) and magnetite, even if all of the aqueous Pu were present as Pu(III). This is consistent with solubility equilibrium between PuO_2(am) and magnetite not controlling the aqueous Pu concentrations in the presence of Eu/Nd. However, the analyses of Set III samples (Figure 6), which were conducted at different added PuO_2(am) concentrations, indicates that the total concentration of solubilized Pu does not depend upon the concentration of PuO_2(am). This observation indicates a possible solubility control on the aqueous Pu concentrations rather than a dependence on adsorption/desorption processes. In this regard, it was also shown (data not given) that the soluble Pu concentrations were independent of the order in which Eu/Nd or Fe(II) were added to the PuO_2/magnetite suspensions. Hence it is possible that a solubility-controlling phase containing Pu(III) formed in these suspensions at high pH. However, if such a phase formed it must be present at low concentration, perhaps a surface precipitate, since XAFS spectroscopic analysis indicates that the Pu precipitate is primarily Pu(IV) with no evidence for the incorporation of Pu(III) in the solid. However, XANES spectroscopy is not very sensitive to the presence of Pu(III) (detection limit 5–10% Pu(III)). Hence a small amount of Pu(III) could still be present at the surface and not detectable by XANES. The XAFS shows the characteristic pattern for PuO_{2+x}, with a clear Pu–Pu backscatter at about 3.80 Å. The relative peak heights of the Pu–O (2.3–2.4 Å) and Pu–Pu backscatters are also very close to those observed previously for PuO_{2+x} precipitates in NaCl solutions.[29] No anomalous features are observed in this sample compared to what would be expected for PuO_{2+x}. TEM analysis of the highest pH sample with added Eu (pH = 6.841, 321 days; Table S6) shows the occurrence of distinct particles of PuO_2(am), magnetite, and $Eu(OH)_3$. The formation of $Eu(OH)_3$ is expected given the high pH and the high total Eu(III) concentration.

The results clearly demonstrate that predicting or modeling the reductive dissolution of PuO_2 is complicated by the possible occurrence of a Pu(III)-containing phase on the surface of PuO_2, in addition to the well-known issues concerning radiolysis. Whether the two phenomena are linked is not known presently. Spectroscopic and microscopic confirmation of the presence and composition of such a phase is a difficult, but important, challenge in the development of mechanistic models for predicting the aqueous concentrations of Pu under

reducing conditions at environmentally relevant circumneutral pH values.

■ ASSOCIATED CONTENT

Supporting Information

Tables of data as mentioned in the text. This material is available free of charge via the Internet at http://pubs.acs.org.

■ AUTHOR INFORMATION

Corresponding Author

*E-mail: ar.felmy@pnnl.gov.

Notes

The authors declare no competing financial interest.

■ ACKNOWLEDGMENTS

This work was supported by the U.S. Department of Energy's Office of Biological and Environmental Research, as part of the Subsurface Biogeochemical Research (SBR) Science Focus Area (SFA) at the Pacific Northwest National Laboratory. A portion of this research was performed using EMSL, a national scientific user facility sponsored by the U.S. Department of Energy's Office of Biological and Environmental Research and located at the Pacific Northwest National Laboratory. We also thank Dr. David Stahl and Professor Ken Czerwinski at the University of Nevada, Las Vegas for facilitating use of the FEI Tecnai $G^2$30 TEM.

■ REFERENCES

(1) Choppin, G. R.; Morgenstern, A. Distribution and movement of environmental plutonium. In *Plutonium in the Environment*; Kudo, A., Ed.; Elsevier Science: Amsterdam, Netherlands, 2001; Vol. *1*, pp 91−105.

(2) Runde, W.; Efurd, D.; Neu, M. P.; Reilly, S. D.; VanPelt, C.; Conradson, S. D. Plutonium in the environment: Speciation, solubility, and the relevance of Pu(VI). In *Plutonium Futures-The Science*; Pillay, K. K. S., Kim, K. C., Eds.; 2000; Vol. *532*, pp 272−273.

(3) Silva, R. J.; Nitsche, H. Environmental Chemistry. In *Advances in Plutonium Chemistry 1967−2000*; Hoffman, D. C., Ed.; American Nuclear Society, University Research Alliance: La Grange Park, IL, Amarillo, TX, 2002.

(4) Kirsch, R.; Fellhauer, D.; Altmaier, M.; Neck, V.; Rossberg, A.; Fanghänel, T.; Charlet, L.; Scheinost, A. C. Oxidation state and local structure of plutonium reacted with magnetite, mackinawite, and chukanovite. *Environ. Sci. Technol.* **2011**, *45* (17), 7267−7274.

(5) Powell, B. A.; Fjeld, R. A.; Kaplan, D. I.; Coates, J. T.; Serkiz, S. M. $Pu(V)O_2^+$ adsorption and reduction by synthetic magnetite (Fe_3O_4). *Environ. Sci. Technol.* **2004**, *38* (22), 6016−6024.

(6) Powell, B. A.; Fjeld, R. A.; Kaplan, D. I.; Coates, J. T.; Serkiz, S. M. $Pu(V)O_2^+$ adsorption and reduction by synthetic hematite and goethite. *Environ. Sci. Technol.* **2005**, *39* (7), 2107−2114.

(7) Keeney-Kennicutt, W. L.; Morse, J. W. The redox chemistry of $Pu(V)O_2^+$ interaction with common mineral surfaces in dilute solutions and seawater. *Geochim. Cosmochim. Acta* **1985**, *49* (12), 2577−2588.

(8) Sanchez, A. L.; Murray, J. W.; Sibley, T. H. The adsorption of plutonium-IV and plutonium-V on goethite. *Geochim. Cosmochim. Acta* **1985**, *49* (11), 2297−2307.

(9) Rai, D.; Gorby, Y. A.; Fredrickson, J. K.; Moore, D. A.; Yui, M. Reductive dissolution of PuO_2(am): The effect of Fe(II) and hydroquinone. *J. Solution Chem.* **2002**, *31* (6), 433−453.

(10) Felmy, A. R.; Moore, D. A.; Rosso, K. M.; Qafoku, O.; Rai, D.; Buck, E. C.; Ilton, E. S. Heterogeneous reduction of PuO_2 with Fe(II): Importance of the Fe(III) reaction product. *Environ. Sci. Technol.* **2011**, *45* (9), 3952−3958.

(11) Grambow, B.; Smailos, E.; Geckeis, H.; Muller, R.; Hentschel, H. Sorption and reduction of uranium(VI) on iron corrosion products under reducing saline conditions. *Radiochim. Acta* **1996**, *74*, 149−154.

(12) Ferriss, E. D. A.; Helean, K. B.; Bryan, C. R.; Brady, P. V.; Ewing, R. C. UO_2 corrosion in an iron waste package. *J. Nucl. Mater.* **2009**, *384* (2), 130−139.

(13) Baer, D. R.; Grosz, A. E.; Ilton, E. S.; Krupka, K. M.; Liu, J.; Penn, R. L.; Pepin, A. Separation, characterization and initial reaction studies of magnetite particles from Hanford sediments. *Phys. Chem. Earth* **2010**, *35* (6−8), 233−241.

(14) Pearce, C. I.; Qafoku, O.; Liu, J.; Arenholz, E.; Heald, S. M.; Kukkadapu, R. K.; Gorski, C. A.; Henderson, C. M. B.; Rosso, K. M. Synthesis and properties of titanomagnetite ($Fe_{3-x}Ti_xO_4$) nanoparticles: A tunable solid-state Fe(II/III) redox system. *J. Colloid Interface Sci.* **2012**, *387*, 24−38.

(15) Liu, J.; Pearce, C. I.; Qafoku, O.; Arenholz, E.; Heald, S. M.; Rosso, K. M. Tc(VII) reduction kinetics by titanomagnetite ($Fe_{3-x}Ti_xO_4$) nanoparticles. *Geochim. Cosmochim. Acta* **2012**, *92* (0), 67−81.

(16) Guigue-Millot, N.; Champion, Y.; Hytch, M. J.; Bernard, F.; Begin-Colin, S.; Perriat, P. Chemical heterogeneities in nanometric titanomagnetites prepared by soft chemistry and studied ex situ: Evidence for Fe-segregation and oxidation kinetics. *J. Phys. Chem. B* **2001**, *105* (29), 7125−7132.

(17) Perriat, P.; Fries, E.; Millot, N.; Domenichini, B. XPS and EELS investigations of chemical homogeneity in nanometer scaled Ti-ferrites obtained by soft chemistry. *Solid State Ionics* **1999**, *117* (1−2), 175−184.

(18) Stookey, L. L. Ferrozine - A new spectrophotometric reagent for iron. *Anal. Chem.* **1970**, *42* (7), 779−781.

(19) Wilson, R. E.; Skanthakumar, S.; Soderholm, L. Separation of plutonium oxide nanoparticles and colloids. *Angew. Chem., Int. Ed.* **2011**, *50* (47), 11234−11237.

(20) Mitchell, D. R. G.; Schaffer, B. Scripting-customised microscopy tools for Digital Micrograph(TM). *Ultramicroscopy* **2005**, *103* (4), 319−332.

(21) Martell, A. E.; Smith, R. M. *NIST Critically Selected Stability Constants of Metal Complexes*; *NIST Standard Reference Database 46 Version 7.0*; Gaithersburg, MD, 2003.

(22) Stefánsson, A. Iron(III) hydrolysis and solubility at 25 °C. *Environ. Sci. Technol.* **2007**, *41* (17), 6117−6123.

(23) Robie, R. A.; Hemingway, B. S. *Thermodynamic Properties of Minerals and Related Substances at 298.15 K and 1 bar (10^5 Pascals) Pressure and at Higher Temperatures*; U.S. Geological Survey: Denver, CO, 1995.

(24) Felmy, A. R.; Rai, D. Application of Pitzer's equations for modeling the aqueous thermodynamics of actinide species in natural waters: A review. *J. Solution Chem.* **1999**, *28* (5), 533−553.

(25) Lemire, R. J. *Chemical Thermodynamics of Neptunium and Plutonium*; Elsevier: Nuclear Energy Agency (NEA) Data Bank, Organisation for Economic Co-operation and Development: North-Holland, Amsterdam, Oxford, 2001.

(26) Felmy, A. R. GMIN: A computerized chemical equilibrium model using a constrained minimization of the Gibbs Free Energy: Summary report. In *Chemical Equilibrium and Reaction Models*; SSSA Special Publication 42; Loeppert, R. H., Schwab, A. P., Goldberg, S., Eds.; Soil Society of America: Madison, WI, 1995.

(27) Guillaumont, R.; Fanghänel, T.; Fuger, J.; Grenthe, I.; Neck, V.; Palmer, D. A.; Rand, M. H. *Update on the Chemical Thermodynamics of Uranium, Neptunium, Plutonium, Americium and Technetium*; Elsevier: Amsterdam, 2003; p 919.

(28) Neck, V.; Altmaier, M.; Fanghänel, T. Solubility of plutonium hydroxides/hydrous oxides under reducing conditions and in the presence of oxygen. *C. R. Chim.* **2007**, *10* (10−11), 959−977.

(29) Ding, M.; Conca, J. L.; den Auwer, C.; Gabitov, R. I.; Hess, N. J.; Paviet-Hartmann, P.; Palmer, P. D.; LoPresti, V.; Conradson, S. D. Chemical speciation of heterogeneously reduced Pu in synthetic brines. *Radiochim. Acta* **2006**, *94* (5), 249−259.

(30) Rai, D.; Felmy, A. R.; Fulton, R. W. Nd^{3+} Am^{3+} ion interactions with sulfate ion and their influence on $NdPO_4(c)$ solubility. *J. Solution Chem.* **1995**, *24* (9), 879−895.
(31) Felmy, A. R.; Wang, Z.; Dixon, D. A.; Joly, A. G.; Rustad, J. R.; Mason, M. J. The aqueous complexation of Eu(III) with organic chelates at high-base concentration: Molecular and thermodynamic modeling results. In *Nuclear Site Remediation: First Accomplishments of the Environmental Management Science Program*; ACS Symposium Series 778; Eller, G., Heineman, W. R., Eds.; American Chemical Society: Washington, DC, 2001.